Article

A Hybrid Traffic Sensor Deployment Model with Communication Consideration for Highways

Xing Tong [1], Ming Li [2] and Zhichao Cui [3,*]

1   School of Information Engineering, Chang'an University, Middle-Section of Nan'er Huan Road,
    Xi'an 710064, China; 18560169833@163.com
2   School of Transportation Engineering, Shandong Jianzhu University, No. 1000 Fengming Road, Lingang
    Development Zone, Jinan 250101, China; liming20@sdjzu.edu.cn
3   School of Electronics and Control Engineering, Chang'an University, Middle-Section of Nan'er Huan Road,
    Xi'an 710064, China
*   Correspondence: cui.zhichao@chd.edu.cn

Abstract: This paper mainly studies the deployment of hybrid sensors on highways. By constructing the deployment location constraint model, the overall accuracy of sensor deployment can be maximized. In addition, in order to meet the needs of intelligent transportation, the consideration of traffic data communication is added to the work. The highway under study is first divided into several units, and the combination type of sensors is used to represent the possible layout of two adjacent sensors. Then, a 0–1 optimization model reflecting the interaction between the sensor position and the server position is established. Then, a two-step search algorithm is proposed to find the optimal solution of the model and determine the deployment scheme with maximum accuracy. Finally, an example is given to verify the method. The results show that there are significant differences between uniform unit-deployment schemes and non-uniform unit-deployment schemes. Through the sensitivity analysis of each factor, the influence of budget and communication radius on the deployment plan is proven. In addition, the ramp length can also have a negative impact on the target value.

Keywords: hybrid sensors; highway; deployment; communication

1. Introduction

With the development of autonomous vehicles and wireless communication technology, people have paid more attention to the daily travel experience, such as planning travel paths precisely and broadcasting travel information dynamically. These idealized scenes not only impose requirements on vehicles but also need the coordination of advanced infrastructures to achieve this goal. This is because traffic managers have to gather a variety of information to make efficient decisions. Traffic data are the foundation of transportation planning and operational activities and can be collected by devices in-vehicle or on the roadside. Managers monitor traffic mainly through data recorded from fixed sensors on the roadside. Since sensors cannot be installed in the whole transportation network, the supervision of partial roads must rely on traffic theory and infer traffic states. In this circumstance, it becomes a challenge to estimate traffic system performance accurately.

To give significant suggestions on this issue, lots of effort has been spent on investigating the optimal deployment of sensors. Most of them hope to maximize performance measures of selected roads with fewer sensors. For example, Li et al. [1] proposed a model to optimally deploy roadside units, which aims at minimizing the worst-case system travel time with a given budget. Danczyk et al. [2] focused on the effect of sensor failures on the sensor location model by minimizing average incurred error. Fu et al. [3] established a two-stage model to minimize the total number of sensors and make cost-effective strategies for sensor deployment. Among these studies, there are many types of sensors adopted to

monitor traffic, such as loop detectors, RSUs (Road Side Units), cameras, laser sensors, and ultra-acoustic sensors. Due to differences in sensor attributes (e.g., cost, service scope, data type), they have their own advantages in application. Traffic flow observation [4,5], travel time estimation [6,7] and path reconstruction [8] are universal goals to conduct the work of optimizing sensor locations. To improve the evaluation accuracy, mixed types of sensors may also be taken into consideration to enrich traffic information [9]. These assumptions are usually used in the background of freeways or urban road networks to discuss the sensor location problem. Danczyk and Liu [10] focused on the allocation of loop detectors along freeway corridors. Kim et al. [11] investigated travel time estimation by optimizing the placement and density of point sensors in a freeway. Li et al. [12] studied the roadside sensor placement problem to monitor the state of a traffic network. Salari et al. [13] tried to reach full link-flow observability to optimize sensor configuration in a traffic network. Gentili and Mirchandani [14] discussed the problem of optimally locating sensors on a traffic network.

In most studies, the location problem of mixed types of sensors on the highway has received less attention. This problem has been discussed well for traffic networks [9,15,16]. These works provide valuable directions to predict traffic flow or OD (Origin Destination) matrices. However, in addition to traffic state prediction, road managers also need to pay attention to real-time information broadcasting in the future intelligent transportation system. The extraction of some traffic information might be time-consuming, which is expected to be executed in local servers instead of transmitting data to the control center. Against this background, the idea of edge computing is widely introduced to save computing time and reduce communication delay. Thus, the deployment of edge computing infrastructure should be considered when planning the location of sensors. In recent years, numerous works on the problem of server placement have been proposed. Among them, the constraint of workload and computing capacity are mainly considered in the optimization model [17–20]. And the objective for the problem mainly includes energy consumption [21], workload balancing [22], and the total cost [23,24]. To avoid the effect of traffic data storage and processing on the sensor deployment problem, this paper intends to investigate it by integrating the problem of server placement for highways. Therefore, this paper will propose an optimization model and design an efficient method to solve this challenge. The main contributions of this paper can be concluded as follows.

1. This paper considers the location of multi-type sensors when discussing the sensor-deployment problem along highways.
2. This paper takes the problem of computing server placement into consideration to meet the demand of realizing the construction of intelligent transportation systems.
3. This paper studies the hybrid traffic sensor deployment problem with communication consideration by formulating a binary optimization model and designing a heuristic algorithm.

The remainder of this paper is organized as follows: Section 2 illustrates the sensor deployment problem and formulates it into a mathematical model. Section 3 introduces the solution algorithm for the hybrid sensor deployment problem. Case studies and conclusions are presented in Sections 4 and 5, respectively.

2. The Optimization Model for the Hybrid Sensor Deployment

This paper assumes that two kinds of sensors will be deployed along the researched highway, i.e., RSUs and camera sensors. As listed in Table 1, cameras can capture videos of the highway environment, which are utilized to extract information on traffic flow, traffic density, and vehicle trajectory. Meanwhile, RSUs can acquire information on vehicle speeds and vehicle positions recorded in the text. For the convenience of stating the multi-type sensor-deployment problem, the highway is divided into several uniform cells, as shown in Figure 1. Four combination types could be listed for two adjacent sensors, i.e., {camera, camera}, {camera, RSU}, {RSU, camera}, and {RSU, RSU}, which are labeled as types 1, 2, 3, and 4, respectively, as shown in Table 2. With this configuration, the problem can be

regarded as selecting appropriate cells to install sensors and combination types to monitor the researched road. Since sensors located along the road are not only used to capture traffic information of designated points, monitoring traffic conditions of the entire road by integrating traffic data from multiple sensor points is more meaningful for traffic managers. Thus, the monitoring efficiency of the area between two adjacent sensors becomes a critical indicator for evaluating sensor-deployment plans. To express the model in a simplified way, a binary coefficient π_{ij}^k is defined and denoted as the accuracy rate from cell i to j via the kth combination type of hybrid sensor. Therefore, the multi-type sensor-deployment problem will be converted into finding optimal combination types.
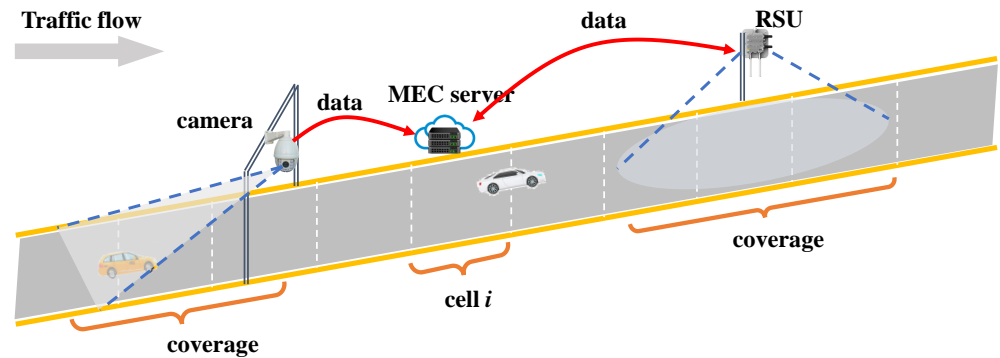

Figure 1. A sketch map of sensor layout.

Table 1. The data information for roadside equipment.

Equipment	Transferred Information	Format
RSU	vehicle speed vehicle position	text
Camera	traffic flow traffic density vehicle trajectory	text video

Table 2. The type of required sensors and servers.

		Cell i	
		Camera	**RSU**
Cell j	Camera	type 1	type 2
	RSU	type 3	type 4

Based on the above assumption, the optimization model of the multi-type sensor deployment problem will be introduced as follows. For a researched road with $N = \{1, 2, 3, \ldots, N\}$ cells, the length of each cell is Δd, and sensors are assumed to be deployed in the middle of designated cells. The total investment cost is W. The unit cost of each RSU and camera is, respectively, w_r and w_c. The set of combination types is S, where $S = \{1, 2, 3, 4\}$. Since directly sending video data to the control center usually takes some time, the idea of Multi-access Edge Computing (MEC) is widely adopted to preprocess data and reduce latency. The MEC server is one of the essential parts of complete edge computing. Thus, the number and location of MEC servers also need to be considered. Similar to locating sensors, the main concern of the MEC server-deployment problem is to search for the proper placement of cells. Therefore, two binary variables x_{ij}^k ($\forall i, j \in N, k \in S$) and z_u ($\forall u \in N$) are applied to formulate the researched problem, where x_{ij}^k is equal to 1 if the region between cell i and j is monitored via the kth combination type of sensors, and z_u is equal to 1 if an MEC server is located in the middle of cell u. The process of decoding variable x_{ij}^k to obtain sensor location can be explained with the example shown in Figure 2. It should be noted that cells

0 and $n + 1$ are two dummy cells, which are used to represent the origin and destination cells. The basic idea is to find those (i, j) pairs making $\sum_{(k \in S)} \forall x_{ij}^k$ equal to 1. Feasible pairs of Figure 2 are labeled with red dashed lines. These dash lines joined together are similar to a smooth trajectory, where the destination cell of a dashed line is the origin cell of its downstream line. Sensors are selected to be deployed at the junction of two adjacent lines. So for each dashed line, it implies that the origin and destination cell of this line should be placed with sensors, i.e., cells 3, 7, and m equipped with sensors. According to the characteristic of variable x_{ij}^k, some constraints related to trajectory optimization should be added. With these considerations, the objective function and constraints of the multi-sensor deployment will be stated.
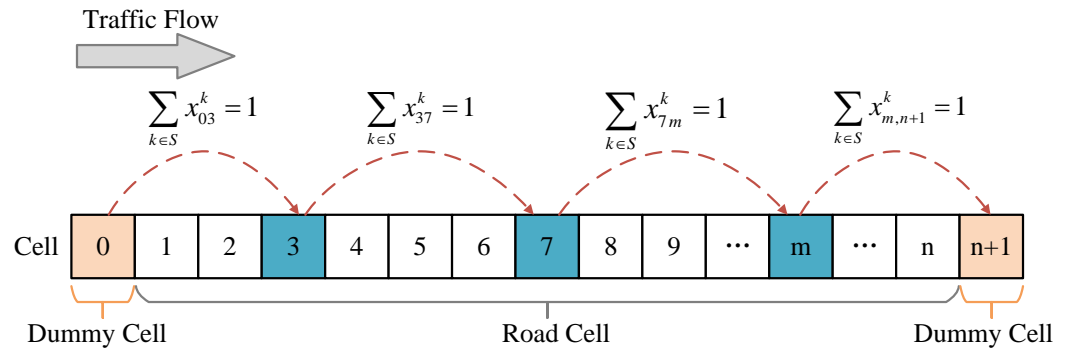

Figure 2. An example of finding sensors' location.

The main objective of this paper is to maximize the accuracy rate of monitoring traffic scenes, which can be briefly stated as Equation (1).

$$max \sum_{i,j \in N \cup \{0,n+1\}, k \in S} \pi_{ij}^k x_{ij}^k \tag{1}$$

where 0 and $n + 1$ represent two dummy cells. To make solutions feasible, constraints for sensor and sever location are detailedly described as follows.

(1) Dummy cell constraint

Information flow in the network flows from the start cell to the target cell, so the direction of information transmission and traffic flow are fixed. Constraints need to be added to ensure that the trajectory starts from 0 and ends with $n + 1$. Equation (2) guarantees that feasible trajectories need start at dummy cell 0 and end at dummy cell $n + 1$, as shown in Figure 2.

$$\sum_{k \in S, j \in N \cup \{n+1\}} x_{0j}^k = 1$$
$$\sum_{k \in S, i \in N \cup \{0\}} x_{i,n+1}^k = 1 \tag{2}$$

(2) Road cell constraint

Since sensors will not be placed on all road cells, a feasible trajectory could only contain partial road cells. For simplicity, it is assumed that each cell is equipped with one sensor at most. In fact, a monitor point along the road might use several sensors. Although Equation (3) does not satisfy all scenarios, it can be modified if necessary. This paper first formulates the model under a simple scenario, and a cell with multiple sensors will be considered as extended research.

$$\sum_{k \in S, j \in N - \{i\}} x_{ij}^k \leq 1, \forall i \in N \tag{3}$$

In addition, Equation (4) is added to avoid generating a detour trajectory. It implies that a trajectory should move along the direction of traffic flow.

$$\sum_{k\in S, j\in\{1,2,\dots,i-1\}} x_{ij}^k = 0, \forall i \in N \tag{4}$$

Except for eliminating detour, the consistency of a trajectory should also be considered, which is stated as Equation (5). It indicates that if a road cell is a destination cell of a trajectory, it must be an origin cell of another trajectory. To meet this requirement, an auxiliary parameter Ω^k represents the set of connective combination types of the kth combination type. For example, if the combination type {camera, camera} is selected, the following combination type should be {camera, camera} or {camera, RSU}. So, for $k = 1$, the connective set Ω^1 is equal to $\{1, 2\}$.

$$\sum_{i\in N} x_{ij}^k = \sum_{i\in N, m\in\Omega^k} x_{ji}^m, \forall j \in N, k \in S \tag{5}$$

(3)   Investment cost constraint

With economic considerations, the total cost of sensors and MEC servers should not be larger than the budget W, as shown in Equation (6). It should be noted that c^k denotes the first sensor cost of combination type k. For example, c^1 is equal to w_c . Since the first sensor of type 1 is the camera, the value of c^1 should be equal to the cost of the camera.

$$\sum_{i,j\in N\cup\{n+1\}, k\in S} c^k x_{ij}^k + \sum_{u\in N} \varpi z_u \leq W \tag{6}$$

where ϖ is the unit cost of an MEC server.

(4)   Capacity constraint

Since the data-processing time is limited by an MEC server's capacity, multiple sensors send requirements simultaneously to a server, which might bring about a negative effect on computation speed. To improve computational efficiency and reduce latency, the number of sensors associated with a server is constrained, as shown in Equation (7).

$$\sum_{i\in N} y_{iu} \left(\sum_{j\in N, k\in S} \alpha_k x_{ij}^k \right) \leq z_u F, \forall u \in N \tag{7}$$

where α_k represents the required storage space of the first sensor of combination type k, F denotes the capacity of an MEC server, y_{iu} utilizes a binary value to represent the service relationship between sensors in location i and servers in location u cell. Equation (8) expresses the connection between the locations of sensors and servers.

$$\sum_{j\in N, k\in S} x_{ij}^k = \sum_{u\in N} y_{iu}, \forall i \in N \tag{8}$$

Equation (9) implies that only if a server is deployed at cell u, the value of y_{iu} can be equal to 1.

$$\sum_{i\in N} y_{iu} \leq z_u M, \forall u \in N \tag{9}$$

Equation (10) indicates the constraint of the service scope of a server.

$$y_{iu} \leq \lambda_{iu}, \forall i, u \in N \tag{10}$$

where λ_{iu} is a $0-1$ index, 1 if cell i is included in the service scope of an MEC server placed on cell u and 0; otherwise, M is a very large number.

(5)   Binary constraint

Equation (11) imposes the binary constraints for variables x_{ij}^k, z_u, and y_{iu}.

$$x_{ij}^k \in \{0,1\}, \forall k \in S, i, j, \in N \cup \{0, n+1\}$$
$$z_u \in \{0,1\}, \forall u \in N$$
$$y_{iu} \in \{0,1\}, \forall i, u \in N$$

(11)

Therefore, the entire formulation of the hybrid sensor deployment is outlined as follows.

$$max \sum_{i,j \in N \cup \{0,n+1\}, k \in S} \pi_{ij}^k x_{ij}^k$$
$$s.t. \quad Equations \quad (2) \sim (11)$$

(12)

3. The Solution Algorithm for the Hybrid Sensor Deployment

In the model proposed above, Equation (7) is a nonlinear form to express the capacity constraint, which makes the model unable to be solved in polynomial time. In Equation (7), the term $\sum_{j \in N, k \in S} \alpha_k x_{ij}^k$ denotes the expected computational load of cell i. If it is pre-determined, the optimization model can be easily solved with commercial solvers. This value is highly related to variable x_{ij}^k. It is obvious that the computational load of cell i can be estimated only when the multi-sensor deployment plan is given. Under this condition, the valuable solutions can be determined by respectively finding cells to install sensors and servers through the optimization model. The basic idea is to divide the solving process into two steps. In step I, the algorithm will first determine variable x_{ij}^k and then explore z_u with budget and capacity constraints. In step II, the algorithm will enumerate potential locations for servers and then solve a sub-model with the service scope constraint to obtain variable x_{ij}^k. Since the expected budget is another critical constraint for each step, the algorithm intends to search for more feasible solutions by adjusting the total budget allocation. The framework of the algorithm is depicted in Figure 3. A detailed explanation is introduced as follows.

3.1. The Solution Procedure of Step I

The main idea of this section is to find a feasible deployment plan by solving two sub-models, where sub-model I is used to determine variable x_{ij}^k and sub-model II is adopted to achieve variables y_{iu} and z_u. Since the purpose of solving sub-model I is to give a multi-sensor deployment plan as a reference, only constraints related to sensors are involved (Equations (2)~(5)). In addition, the budget constraint for sensors should be considered. Thus, the formulation of sub-model I is stated as follows.

$$min \sum_{i,j \in N \cup \{0,n+1\}, k \in S} \tilde{\pi}_{ij}^k x_{ij}^k$$
$$s.t. \quad Equations (2) \sim (5)$$
$$\sum_{i,j \in N \cup \{n+1\}, k \in S} c^k x_{ij}^k \leq \omega_1$$

(13)

where ω_1 varies with parameter β (in Figure 3).

With results derived from the above model, the next step is to estimate computation loads f_i for each cell, which provides useful information for placing computing servers on valuable sites. Based on parameter f_i, sub-model II can be formulated as follows.

$$min \sum_{i,u \in N} \phi_{iu} y_{iu}$$

$$s.t. \sum_{u \in N} \varpi z_u \leq W - \omega_1$$

$$\sum_{i \in N} y_{iu} f_i \leq z_u F, \forall u \in N \tag{14}$$

$$Equations \; (8) \sim (10)$$

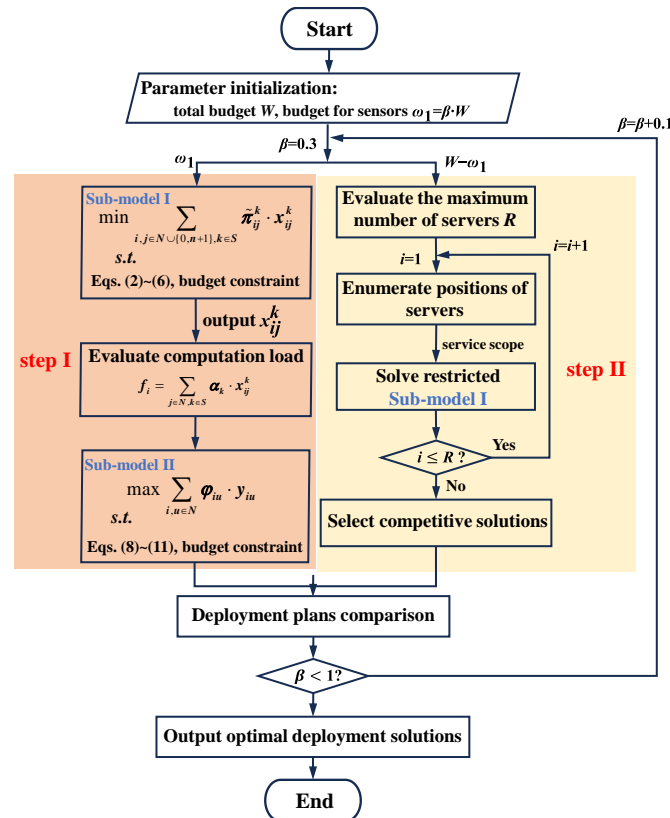where ϕ_{iu} is the distance between cells i and u.

Figure 3. The framework of the proposed solution algorithm.

The above model is a linear expression that can be easily solved by commercial solvers. In this way, the number and location of sensors and servers can be determined. This solution method intends to relax the hard constraint (Equation (7)), while the interaction between servers "location and sensors" site selection is not reflected. This part only imposes the influence of variable x_{ij}^k on variables y_{iu} and z_u. There is a lack of discussion on the reverse relationship. So it is necessary to investigate how to determine the variable x_{ij}^k by presetting the value of z_u. Step II of the proposed solution algorithm is used to complete this task, which will be explained in the following part.

3.2. The Greedy Search Algorithm for Step II

In this step, the maximum budget for purchasing servers is assumed to be provided in advance, i.e., $W - \omega_1$. According to the unit cost of a server, the maximum number of installed servers could be evaluated. The main purpose of applying the greedy search is to enumerate all possible deployment scenarios and select the optimal one for connecting sensors. If the number and location of servers are decided, the service scope of each server can be defined with the communication range. To increase the utilization of each server, sensors should be placed in specific regions. This situation can be described by modifying

road cell constraints (see Equation (15)). This repression reflects the influence of the service scope on variable x_{ij}^k. By adding Equation (15) into sub-model I, an efficient deployment plan could be derived from the restricted model (Equations (13) and (15)).

$$\sum_{i \in \Lambda^m, j \in N \cup \{n+1\}, k \in S} x_{ij}^k \geq 1, m \in \Delta H \tag{15}$$

where ΔH is the set of servers and Λ^m denotes the set of road cells covered by the mth server. Based on Equation (15) and sub-model I, the procedure of the greedy search algorithm is listed in Algorithm 1.

Algorithm 1: The Greedy Search Algorithm

Input: Set N and S, the total budget W, matrix π, installation cost c and ω, server capacity F, expected memory usage α.

Output: The deployment plan x_{ij}^k and y_i.

1 $R \leftarrow \lfloor \frac{W - w_1}{\omega} \rfloor$
2 $H \leftarrow \{1, 2, \ldots, R\}$
3 $\Theta \leftarrow \varnothing$ //Θ means the set of server locations
4 $\Lambda \leftarrow \varnothing$
5 //Part I: site selection
6 **for** h in H **do**
7   Enumerate all possible positions for h servers and record positions in set Θ_h. //Θ_h means that the set of sever locations contains h elements.
8 **end**
9 //Part II: service scope determination
10 **for** h in H **do**
11   **for** g in Θ_h **do**
12   Calculate the service scope for each server and update set Λ^{hg}.
13   **end**
14 **end**
15 //Part III: comparison of sensor deployment plans
16 **for** h in H **do**
17   **for** g in Θ_h **do**
18   Add set Λ^{hg} into Equation (15) and solve restricted sub-model I.
19   **end**
20 **end**
21 Select the deployment plan with the minimum.

---

4. Case Study

In this section, a 26-km stretch of highway in Jinan City in China (Figure 4) was selected as the background to analyze the results of the hybrid-sensor deployment model. The terrain of this road is not consistent. The first 5 km of this road is relatively steep, and the following 5 km of this road is a tunnel. The other parts are conventional contours that are a little steep or curved. For comparison, this road is divided into several homogeneous cells. The length of each cell is set to be 200 m. The deployment of cameras and RSUs on this highway is discussed. The unit cost of the camera and RSU is set to 1.7×10^3 USD (1.2×10^4 CNY) and 2.8×10^3 USD (2×10^4 CNY). The cost of an MEC server is 2.8×10^4 USD (20×10^4 CNY). The total budget W used for buying sensors and servers should not be larger than 2.1×10^5 USD (1.5 million CNY). The average coverage range of an MEC server is within 1 km.

The accuracy rate of each combination type k is assumed to be satisfied with the following piecewise function, which varies with the distance R_{ij} between two adjacent sensors. Figure 5 shows the curves of the accuracy rate of four combination types. When

the distance R_{ij} is larger than the critical distance, values of four curves will fluctuate around 0.

Figure 6 illustrates an example of employing Equation (16) to evaluate the accuracy rate on a road with 100 cells.

$$\tau_{ij}^k = \begin{cases} \theta^k, & 0 < R_{ij} < R_c^k \\ \frac{\theta^k}{1+\exp^{u_k R_{ij}}}, & R_c^k < R_{ij} \end{cases} \tag{16}$$

where θ^k denotes the maximum accuracy rate of combination type k, and R_c^k implies the critical distance. It reflects the impact of cells contained between two sensors on monitoring accuracy. If the number of contained cells is less than 20 (the yellow area in Figure 6), the accuracy rate is higher than 0.8. With the increase in filled cells, the accuracy rate will be gradually reduced to 0.2.
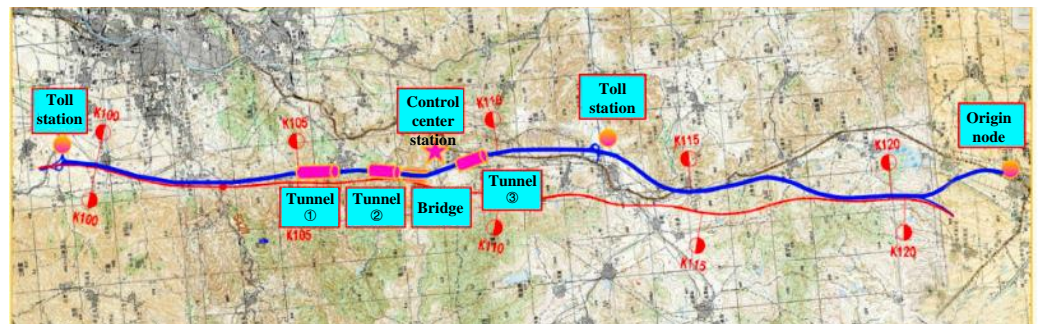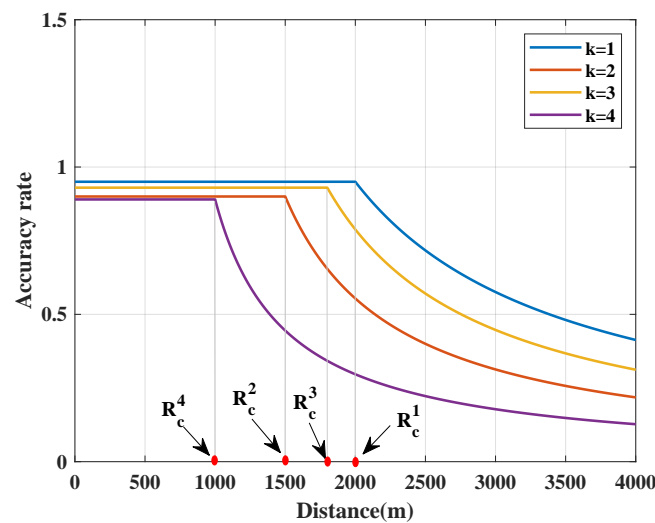

Figure 4. The contour of the research highway.

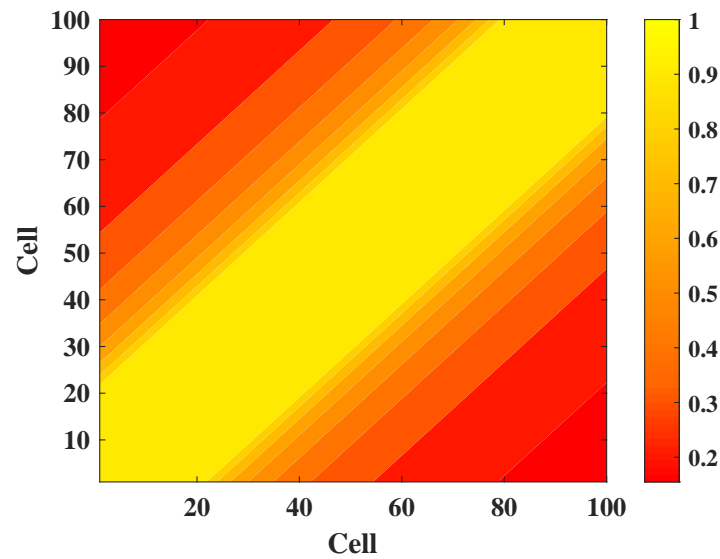**Figure 5.** Accuracy curves of four combination types.

Figure 6. The accuracy rate distribution of 100 cells.

4.1. Deployment Plans of the Homogeneous Highways

In this case study, 100 cells are divided for deployment, and this is labeled as scenario I. It is assumed that each cell is identical and the accuracy rate of monitoring traffic is only influenced by the number of cells. The deployment plan is shown in Figure 7. The total number of cells selected to install sensors is 23, where 20 cells are for cameras and 3 cells are for RSUs. In Figure 7, the green block represents the position of deploying MEC servers. It can be seen that cells 7, 23, 31, 73, 74, and 93 are picked to place servers. The service scope of each server is also depicted. For example, the server placed at cell 7 is used to connect sensors of cell 1 to 13, and the server at cell 31 is mainly used to serve sensors from cell 25 to 36. With the constraint of capacity and communication range, the number of cells associated with each server is limited. The goal of this paper is to maximize the accuracy rate. As a result, the optimized plan intends to choose the most efficient combination type, i.e., {camera, camera}, which makes the number of cameras more than that of RSUs. Due to the limited budget, three RSUs were arranged in this scheme. If the maximum budget is increased, RSUs might not be used to monitor traffic.
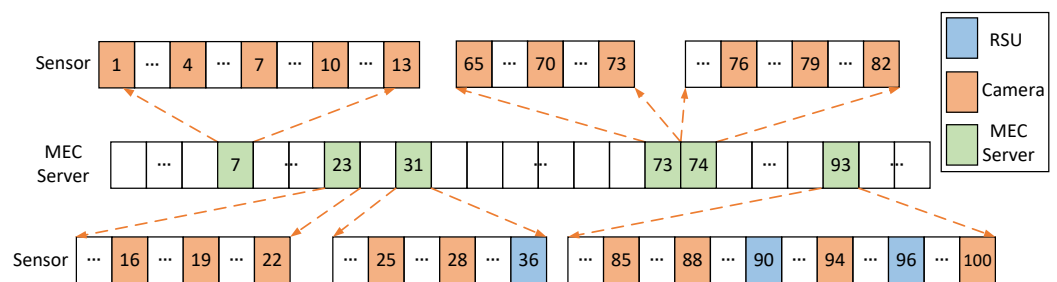

Figure 7. The sensor deployment plan for homogeneous road cells.

In Figure 7, most sensors and servers are deployed at the front and tail cells of the researched highway. There is no budget for installing sensors from cells 37 to 64. Since the cost of the sensor-deployment plan illustrated in Figure 7 is USD 2.1×10^5 (CNY 1.5 million), adding extra sensors from cells 37 to 64 will make the total cost exceed the maximum budget W. This indicates that some cells could not be monitored under this maximum budget, which might be not limited to this region. So Figure 7 shows one of the optimal plans for scenario I. It should be noted that cells 73 and 74 are both selected to install servers. It seems that two servers placed at cell 73 or 74 are more reasonable compared with the optimized plan. Although this might not be considered a profitable plan,

it is in fact acceptable with preset parameters. This is because the communication range is set to be eight. Cell 73 cannot be connected with cell 82 and cell 65 will fail to deliver the message to cell 74. In short, it needs two servers to receive the message delivered from cell 65 to 82.

The goal of increasing the accuracy rate might narrow the distance between two adjacent sensors, which leads to the objective value of some parts being relatively high. This is not beneficial for monitoring the whole region. Hence, the objective function in Equation (11) is modified to balance the accuracy rate and covered regions as follows.

$$max \quad \alpha \sum_{i,j \in N \cup \{0,n+1\}, k \in S} \pi_{ij}^k x_{ij}^k + (1-\alpha) \sum_{i,j \in N \cup \{0,n+1\}, k \in S} \rho_{ij}^k x_{ij}^k, \quad (17)$$

where ρ_{ij}^k denotes the coverage rate and α denotes the weight coefficient. The layouts of sensors in eleven groups of tests when parameter α is changed from 0 to 1 are depicted in Figure 8. The horizontal axis represents the location of sensors (which also can be regarded as labels of road cells), and the vertical axis denotes the value of parameter α. A filled dot indicates a sensor placed at that position. It is obvious that the number of total used sensors is not varied in a wild fluctuation, which is changed over the interval [21, 25]. This implies that parameter α has little impact on the total number of required sensors. Nevertheless, the consistency of deployment plans of these sensors is not high. For example, the beginning and ending cells of $\alpha = 0.4$ are 12 and 100, while occupied cells for $\alpha = 1.0$ range from 66 to 100. Since it is beneficial to increase the accuracy rates of monitoring traffic by shortening the space between two adjacent sensors, the interval between the beginning and ending cells will be narrowed when the value of parameter α is raised. Although the interval in some cases is not significantly reduced, some parts of a deployment plan become more compact. When α is equal to 0.6, 90 cells are covered from the beginning point to the ending point. Compared with those cases (when α is less than 0.6), this interval does not become smaller, but sensors installed from cells 2 to 15 are more compact than the average distance. It should be noted that the optimal gap of the solver is set to 0.3 when considering the computation time. This might make some plans depicted in Figure 8 not optimal. In any case, the results reflect that the distance between two adjacent sensors tends to be closer when the objective function pays more attention to improving the total accuracy rate. For the overall consideration of the accuracy rate and tthe covered regions, $\alpha = 0.5$ is adopted to search for solutions in the following discussions.
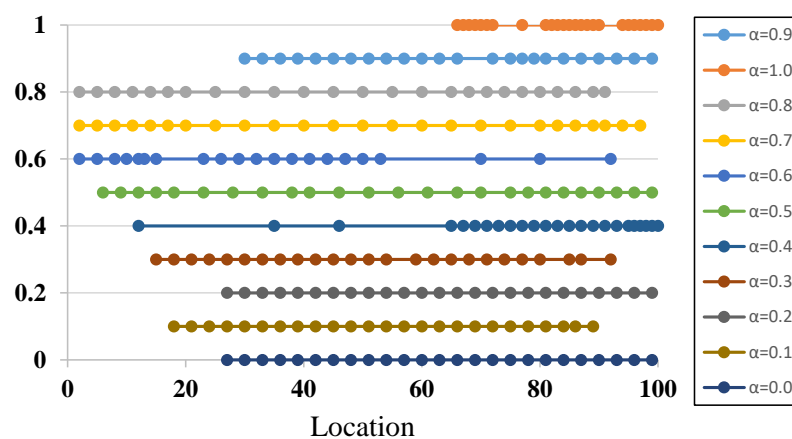

Figure 8. The figure of sensor layout under different weights.

To further analyze the influence of input factors on deployment plans, Figure 9a shows that the numbers of sensors and servers are changed with a preset budget and the communication radius of an MEC server. It can be seen that the budget and communication radii both have a positive impact on the number of used sensors. Enlarging them will lead to an increase in the quantity of buying sensors. The cause of this phenomenon is that more

money could be transferred to purchase sensors. In Figure 9a, this added investment for sensors is attributed to the total budget increase, and it is obtained by cutting down the investment cost of servers in Figure 9b. Since the communication radius is lengthened, an MEC will have the potential of connecting more sensors, which contributes to reducing the number of installed servers. Therefore, the communication radius has a negative influence on the number of servers in Figure 9b. It can be concluded that USD 2.1×10^5 (CNY 1.5 million) budget is more profitable with these settings, and a communication radius of eight cells is sufficient under a budget of USD 2.1×10^5 (CNY 1.5 million).
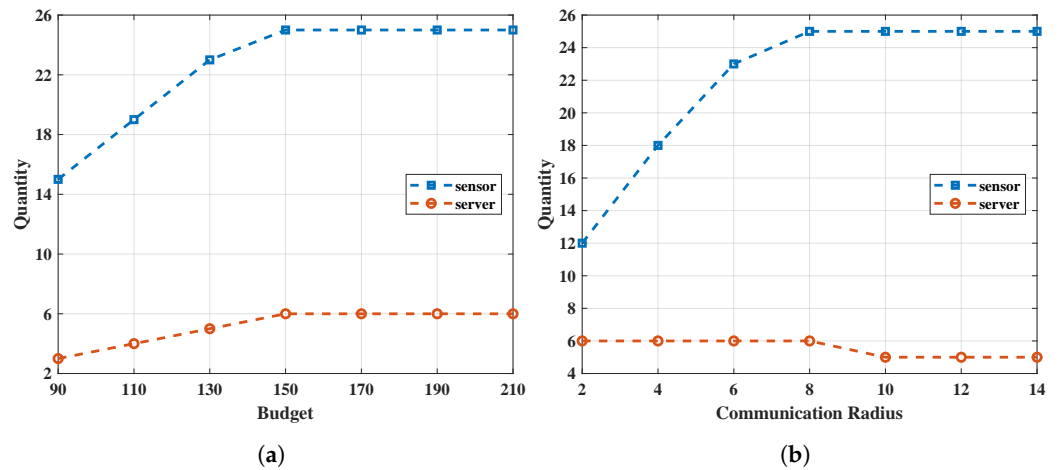

(a)

(b)

Figure 9. The number of servers and sensors varying with the factors of budget and communication radius. (**a**) Budget. (**b**) Communication radius.

4.2. Deployment Plans of the Nonhomogeneous Highway

In addition to straight shapes, curves and slopes are also found along highways, which will decrease the monitored region of a camera and the accuracy rate of traffic prediction. For any combination type, the accuracy rate between two cells not only depends on the distance but is also determined by road shapes. To simulate the researched highway with slopes, the road cells should be nonhomogeneous. Under this circumstance, the evaluation method of accuracy rates still follows the formulation of Equation (17), which is modified by multiplying a coefficient for slope roads. The researched highway is cut into 100 cells, where cells 20 to 35 represent slope roads. The sensor deployment plan for this case is depicted in Figure 10.
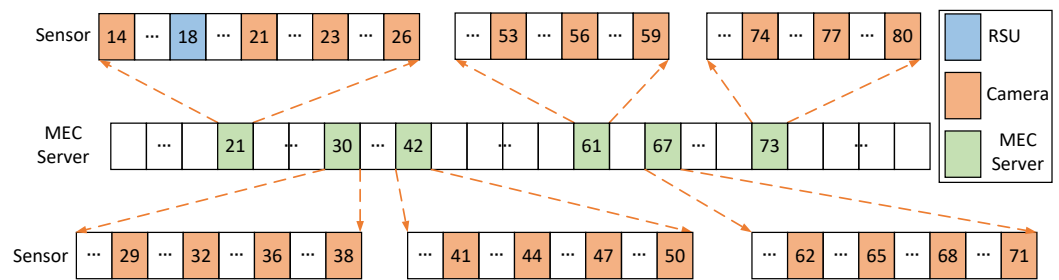

Figure 10. The sensor deployment plan for nonhomogeneous road cells.

The total numbers of used sensors and servers are 23 and 6, respectively. For slope roads, five cameras are installed to monitor traffic. Compared with what is shown in Figure 7, the number of sensors in this region is increased. This is mainly because the distance between two sensors needs to be shortened to maintain the total accuracy rate at a high level. Thus, more sensors should be placed within this zone. It can be seen that the number of required sensors will rise under complicated road conditions. Therefore, the total accuracy rate of the case with sloped roads is a little lower than that of the case

without slope roads. To further analyze the effect of sloped roads on the objective value, a comparison test is conducted for various road lengths (see Figure 11).

In Figure 11, the x-axis represents the ratio of the length of sloped roads to the length of the entire road, where 0 denotes that the entire road is straight without steep slopes and is selected as the benchmark. The left y-axis denotes the total accuracy rate, and the right y-axis denotes the coverage rate. It can be seen that sloped roads would bring a negative influence on the total accuracy rate, especially when the ratio is larger than 0.1. But the accuracy rate did not continuously decline after 0.2 but fluctuated between 18 and 18.5. The coverage rate also showed a downward trend as the ratio increased. It should be noted that a turning point appears at 0.3. Since this test intends to keep the accuracy rate of sloped roads that do not change sharply, the number of sensors within these cells will increase. It might be beneficial for it to improve when the length of slope roads is extended. Table 3 lists the number of required sensors and servers under various ratios. The number of cameras changed from 23 to 25, and the number of RSUs decreased to 0. This is mainly because the prediction accuracy of cameras is supposed to be higher than that of RSUs. More cameras are needed to monitor the traffic on sloped roads. The number of servers varied between five and six. When it was equal to five, the coverage rate could remain unchanged or be increased. This indicates that the distance between two sensors is shortened and that more sensors are clustered by a server.
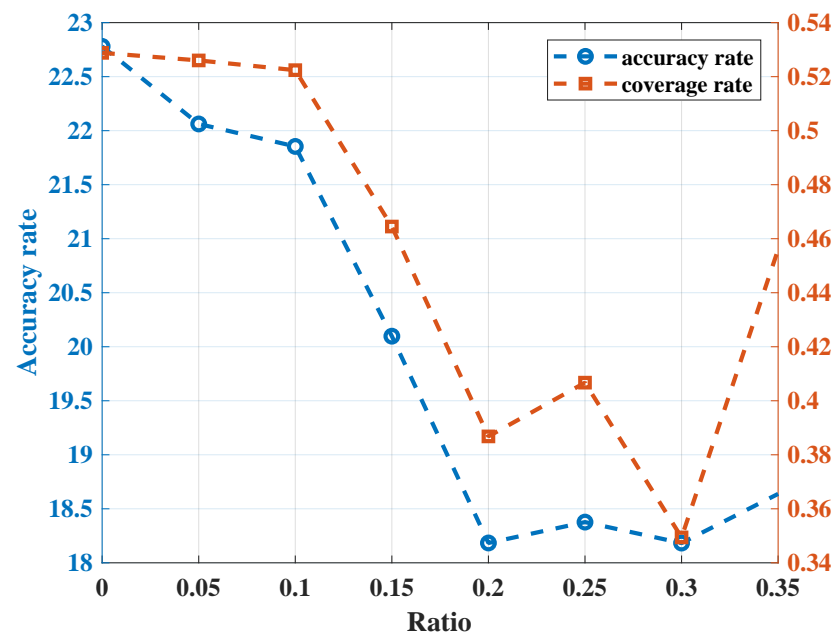

Figure 11. The accuracy rate and coverage rate curves.

Table 3. The number of required sensors and servers.

Equipment	Ratio							
	0	0.05	0.1	0.15	0.2	0.25	0.3	0.35
Camera	20	24	25	25	23	23	25	24
RSU	3	1	0	0	1	1	0	1
Server	6	5	5	6	6	5	6	5

5. Conclusions

This paper investigates the hybrid sensor deployment problem for highways. To fulfill this goal, combination types of sensors are considered as variables, and an arc-based mathematical model is proposed. In the optimization model, the real-time traffic data processing is elaborated by considering the constraint of the MEC server's capacity. Due

to the limitation of computation time, a two-step heuristic search algorithm is adopted to find optimal solutions. This method is tested on the background of a highway in Jinan. The results show that the combination type {camera, camera} is more favored to be selected. The optimal deployment plan is affected by the budget, communication radius, and road shapes. When the budget is given, the total accuracy rate will be decreased by extending the length of sloped roads. Although this paper simultaneously considers the locations of sensors and servers, the connection between servers and sensors is simply stated via the capacity constraint. In future research, the packet loss rate, latency, and other factors could be added to enrich this research. Furthermore, the operating costs of servers and sensors, e.g., energy costs and labor costs, should be considered for evaluating the feasibility of deployment plans. Long-term planning would be more valuable for the hybrid sensor deployment problem, which could be taken into consideration in future studies.

Author Contributions: Conceptualization, X.T.; Methodology, X.T., M.L., Z.C.; Validation, X.T., M.L., Z.C.; Investigation, X.T., M.L., Z.C.; Writing—original draft, X.T., Z.C.; Writing—review and editing, M.L., Z.C.; Supervision, Z.C., X.T. All authors have read and agreed to the published the version of the manuscript.

Institutional Review Board Statement: Not applicable.

Informed Consent Statement: Not applicable.

Data Availability Statement: The data presented in this study are available on request from the corresponding author. The data are not publicly available due to privacy.

Conflicts of Interest: The authors declare no conflicts of interest.

References

1. Li, Y.; Chen, Z.; Yin, Y.; Peeta, S. Deployment of roadside units to overcome connectivity gap in transportation networks with mixed traffic. *Transp. Res. Part C Emerg. Technol.* **2020**, *111*, 496–512. [CrossRef]
2. Danczyk, A.; Di, X.; Liu, H.X. A probabilistic optimization model for allocating freeway sensors. *Transp. Res. Part C Emerg. Technol.* **2016**, *67*, 378–398. [CrossRef]
3. Fu, C.; Zhu, N.; Ling, S.; Ma, S.; Huang, Y. Heterogeneous sensor location model for path reconstruction. *Transp. Res. Part B Methodol.* **2016**, *91*, 77–97. [CrossRef]
4. Owais, M.; Matouk, A.E. A factorization scheme for observability analysis in transportation networks. *Expert Syst. Appl.* **2021**, *174*, 114727. [CrossRef]
5. Xu, X.; Lo, H.K.; Chen, A.; Castillo, E. Robust network sensor location for complete link flow observability under uncertainty. *Transp. Res. Part B Methodol.* **2016**, *88*, 1–20. [CrossRef]
6. Zhu, N.; Ma, S.; Zheng, L. Travel time estimation oriented freeway sensor placement problem considering sensor failure. *J. Intell. Transp. Syst.* **2017**, *21*, 26–40. [CrossRef]
7. Mirchandani, P.B.; Gentili, M.; He, Y. Location of vehicle identification sensors to monitor travel-time performance. *IET Intell. Transp. Syst.* **2009**, *3*, 289–303. [CrossRef]
8. Mínguez, R.; Sánchez-Cambronero, S.; Castillo, E.; Jiménez, P. Optimal traffic plate scanning location for OD trip matrix and route estimation in road networks. *Transp. Res. Part B Methodol.* **2010**, *44*, 282–298. [CrossRef]
9. Hu, S.R.; Peeta, S.; Liou, H.T. Integrated determination of network origin–destination trip matrix and heterogeneous sensor selection and location strategy. *IEEE Trans. Intell. Transp. Syst.* **2015**, *17*, 195–205. [CrossRef]
10. Danczyk, A.; Liu, H.X. A mixed-integer linear program for optimizing sensor locations along freeway corridors. *Transp. Res. Part B Methodol.* **2011**, *45*, 208–217. [CrossRef]
11. Kim, J.; Park, B.B.; Lee, J.; Won, J. Determining optimal sensor locations in freeway using genetic algorithm-based optimization. *Eng. Appl. Artif. Intell.* **2011**, *24*, 318–324. [CrossRef]
12. Li, R.; Mehr, N.; Horowitz, R. Submodularity of optimal sensor placement for traffic networks. *Transp. Res. Part B Methodol.* **2023**, *171*, 29–43. [CrossRef]
13. Salari, M.; Kattan, L.; Lam, W.H.; Lo, H.; Esfeh, M.A. Optimization of traffic sensor location for complete link flow observability in traffic network considering sensor failure. *Transp. Res. Part B Methodol.* **2019**, *121*, 216–251. [CrossRef]

14. Gentili, M.; Mirchandani, P.B. Locating sensors on traffic networks: Models, challenges and research opportunities. *Transp. Res. Part C Emerg. Technol.* **2012**, *24*, 227–255. [CrossRef]

15. Zhou, X.; List, G.F. An information-theoretic sensor location model for traffic origin-destination demand estimation applications. *Transp. Sci.* **2010**, *44*, 254–273. [CrossRef]

16. Castillo, E.; Nogal, M.; Rivas, A.; Sánchez-Cambronero, S. Observability of traffic networks. Optimal location of counting and scanning devices. *Transp. B Transp. Dyn.* **2013**, *1*, 68–102. [CrossRef]

17. Chen, L.; Wu, J.; Zhou, G.; Ma, L. QUICK: QoS-guaranteed efficient cloudlet placement in wireless metropolitan area networks. *J. Supercomput.* **2018**, *74*, 4037–4059. [CrossRef]

18. Jiao, J.; Chen, L.; Hong, X.; Shi, J. A heuristic algorithm for optimal facility placement in mobile edge networks. *KSII Trans. Internet Inf. Syst.* **2017**, *11*, 3329–3350.

19. Xu, Z.; Liang, W.; Xu, W.; Jia, M.; Guo, S. Efficient algorithms for capacitated cloudlet placements. *IEEE Trans. Parallel Distrib. Syst.* **2015**, *27*, 2866–2880. [CrossRef]

20. Lähderanta, T.; Leppänen, T.; Ruha, L.; Lovén, L.; Harjula, E.; Ylianttila, M.; Riekki, J.; Sillanpää, M.J. Edge computing server placement with capacitated location allocation. *J. Parallel Distrib. Comput.* **2021**, *153*, 130–149. [CrossRef]

21. Yang, S.; Li, F.; Shen, M.; Chen, X.; Fu, X.; Wang, Y. Cloudlet placement and task allocation in mobile edge computing. *IEEE Internet Things J.* **2019**, *6*, 5853–5863. [CrossRef]

22. Li, C.; Tang, J.; Luo, Y. Service cost-based resource optimization and load balancing for edge and cloud environment. *Knowl. Inf. Syst.* **2020**, *62*, 4255–4275. [CrossRef]

23. Wang, Z.; Gao, F.; Jin, X. Optimal deployment of cloudlets based on cost and latency in Internet of Things networks. *Wirel. Netw.* **2020**, *26*, 6077–6093. [CrossRef]

24. Li, B.; Hou, P.; Wu, H.; Hou, F. Optimal edge server deployment and allocation strategy in 5G ultra-dense networking environments. *Pervasive Mob. Comput.* **2021**, *72*, 101312. [CrossRef]